AIAA-2001-4205

# ASSESSMENT OF THE PROBABILITY OF A MIDAIR COLLISION DURING AN ULTRA CLOSELY SPACED PARALLEL APPROACH

*Sharon Houck* and J. David Powell†*

*Department of Aeronautics and Astronautics, Stanford University Stanford, CA 94305*

## ABSTRACT

In this era of increasing delays in air travel, all means of increasing the capacity of both airports and airspace are receiving intense consideration. In anticipation of future high precision guidance, navigation, and data link systems being implemented by the FAA, procedures once deemed unsafe are again being scrutinized for feasibility. The procedure addressed in this paper is simultaneous approaches into an airport with parallel runways spaced less than 1500 ft apart. The goal of this work is to determine the necessary technological components for reducing the runway spacing to less than 1500 ft. To assess the probability of collision during any one particular approach, variables such as navigation sensor error, flight technical error, relative longitudinal spacing, relative airspeeds, and data link delay time must all be modeled as probabilistic parameters. This research used Monte Carlo simulations in order to assess the probability of collision. The analysis shows that with a GPS-based Local Area Augmentation System installed and a reliable data link transmitting full state information between aircraft, runway spacing may be safely reduced to less than 1500 ft.

## INTRODUCTION

Commercial air traffic is projected to grow approximately 5% per year over the coming decades. This means that the world's airports and airspace will need to handle an increase of traffic by a factor of two or three over the next two decades. Many airports are near or at capacity now for at least portions of the day. Therefore, it is clear that major increases in airport capacity will be required in order to support the projected growth in air traffic. This can be accomplished by adding airports, adding runways at existing airports, or increasing the capacity of the existing runways. With the current approved technology for the use of multiple runways at an airport under Instrument Meteorological Conditions (IMC), parallel runways must be set at least 3400 ft apart if the airport is equipped with the newest radar. In clear weather (Visual MC or VMC), parallel runways can be used that are 700 ft apart.

*Research Assistant, Member AIAA

†Professor, Fellow, AIAA



If technology can be developed that would allow 750-ft separation between parallel runways in IMC, the capacity of a significant fraction of today's airports would be doubled during IMC. This would be a major benefit to airport capacity with no increased airport land area requirements and thus minimal impact on the surrounding communities. However, in the longer term, technology that allows use of Ultra Closely Spaced (750 ft to 1500 ft) Parallel Approaches (UCSPA) would have a huge beneficial effect on the environmental impact of airport capacity increases. To support airport capacity increases by a factor of two or three over the next two decades, new runways will be required. As the required spacing between runways decreases, the required new land or water fill decreases, thus reducing the environmental impact. The goal of this research is to quantify the effect of improved technology on required runway spacing; specifically, the effects of improvements in navigation enabled by the GPS-based Local Area Augmentation System (LAAS), improvements in guidance through the use of advanced pilot displays, and auto-pilots, and the introduction of new information to pilots on neighboring traffic made possible by data links. These variables are all included in a Monte Carlo evaluation to assess the probability of collision for the parallel approach scenario. These new technologies have already been shown to be effective in limited flight testing. In addition, a new type of auto-pilot, dubbed the "intelligent auto-pilot", is proposed that would improve the reaction times still further. Its effect on collision probabilities and runway spacing is also included.

## PROBABILISTIC STUDIES OF ULTRA CLOSELY SPACED PARALLEL APPROACHES

The generalized sensitivity study of ultra closely spaced parallel approaches presented in [1] was based on deterministic parameters, which in reality are not deterministic, but probabilistic. While appropriate for sensitivity studies, to study the likelihood of collision for any given approach it is necessary to model the probabilistic parameters with representative distributions. The resulting distribution of closest points of approach for thousands of trajectories may then be studied and the probability of collision assessed during a blunder for various approach guidance system/pilot interface combinations. The results may then be combined with an assessment of the probability of a

blunder occurring during an approach to determine the overall likelihood of a collision for any given ultra closely spaced parallel approach.

## PROBABILITY OF COLLISION

Using the results of the sensitivity analysis as well as the approach model, the data presented in [2] on navigation sensor error (NSE) and flight technical error (FTE), and the data from [3] and [4] with respect to pilot response time, a Monte Carlo simulation was created that modeled the FTE, the NSE, the delay time, the relative velocity, and the relative longitudinal spacing as probabilistic variables rather than the deterministic variables of the sensitivity study. Equations derived in [1] were used to propagate the relative aircraft motion in the simulation. For each simulation, it was presumed that the evading aircraft pilot or auto-pilot had enough state information to diagnose the beginning of the blunder, the maximum roll angle and roll rate of the blunderer, and the maximum heading change of the blundering aircraft.

## AIRCRAFT MODEL

In order to more accurately model the aircraft dynamic response for the blunder and evasion maneuvers, linearized aerodynamic coefficients for an older model B-747 were used to create roll input trajectories for a given aileron input for both the evader and blunderer airplanes. Figure 1 presents the geometric and aerodynamic data for the B-747 from [5].

Figure 1. B-747 data

| Parameter | Value |
|---|---|
| $I_x(\text{slug}\cdot\text{ft}^2)$ | 18.2e6 |
| Wing area, S, $\text{ft}^2$ | 5500 |
| Wing span, b, ft | 195.68 |
| $C_{l_p}$ | -0.45 |
| $C_{l_{\delta a}}$ | 0.0461 |

Beginning with the linearized, small perturbation aircraft dynamic equations of motion, assuming x-z plane symmetry and simple roll without perturbation in the other axes:

$$\frac{\partial L}{\partial \delta_a}\Delta\delta_a + \frac{\partial L}{\partial p}\Delta p = I_x\Delta\dot{p} \qquad (1)$$

where L is rolling moment, $\delta_a$ is aileron deflection, p is roll rate, $I_x$ is moment of inertia in the x-plane, and $\dot{p}$ is roll acceleration. $(\partial L/\partial\delta_a)\Delta\delta_a$ is the roll moment due to the deflection of the ailerons and $(\partial L/\partial p)\Delta p$ is the roll-damping moment. Eqn 1) may be rewritten as

$$\tau\Delta\dot{p} + \Delta p = -\frac{L_{\delta a}\Delta\delta_a}{L_p} \qquad (2)$$

where

$$\tau = -\frac{1}{L_p} \quad L_p = \frac{QSb^2C_{l_p}}{2I_x u_0} \quad L_{\delta a} = \frac{QSbC_{l_{\delta a}}}{I_x} \qquad (3)$$

and $\tau$ is defined as the roll mode time constant, Q is the dynamic pressure and $u_0$ is the airspeed. For a step change in aileron deflection, Eqn 2) may be analytically solved to produce

$$\Delta p(t) = -\frac{L_{\delta a}}{L_p}(1 - e^{-t/\tau})\Delta\delta_a \qquad (4)$$

The baseline blunder trajectory for the Monte Carlo runs was the same as that of the sensitivity studies only in order to generate a 10 deg/s roll rate, a step aileron input of 40 deg was specified and the roll rate time history proceeded from Eqn 4). The 40 deg aileron input produced the roll rate time history presented in Figure 2. The roll responses of both the evader and the blundering aircraft were modeled in this way.

Figure 2. Time history of roll angle of modeled B-747 with 40 deg aileron input.

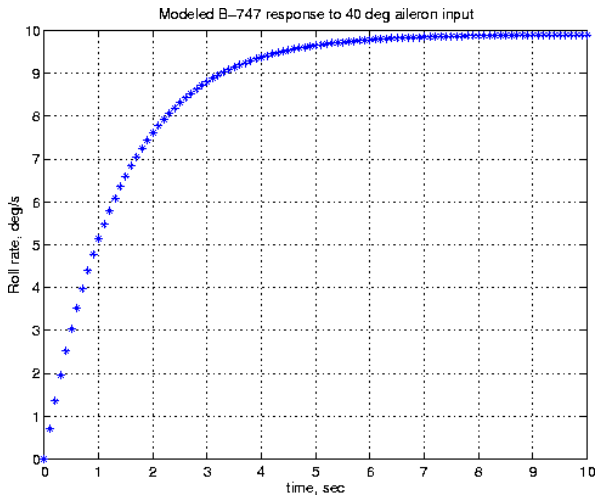


## NAVIGATION SENSOR ERROR MODELS

The navigation sensors used in this study were the Category II Instrument Landing System (ILS) and Local

Area Augmentation System (LAAS), the current and future United States precision approach guidance systems. Each was modeled as a gaussian distribution with the modeled Category II ILS lateral NSE one sigma error being 132 ft and the LAAS one sigma being 4.9 ft. These numbers are based on NSE allowed for a Category II ILS just outside 5nm from the runway threshold and a Category I type of LAAS model at 5nm

The ILS accuracy is driven by its sensitivity to the local environment. Multipath due to hangars, taxiing aircraft, and terrain cause bending or scalloping of the indicated glidepath. Additional interference caused by other radio frequency sources reduce the accuracy of the ILS. The FAA's Standard Flight Inspection Manual defines the procedures for testing the accuracy of the ILS [6]. ICAO standards for ILS accuracy are presented in Figure 3 [7].

Figure 3. ICAO ILS permitted guidance errors

| Approach position | ILS element | Category I | | | Category II | | | Category III | | |
|---|---|---|---|---|---|---|---|---|---|---|
| | | Bias, ft (Max) | Bends, ft (95%) | Total NSE, ft | Bias, ft (Max) | Bends, ft (95%) | Total NSE, ft | Bias, ft (Max) | Bends, ft (95%) | Total NSE, ft |
| Outer Marker (5nm) | Glideslope | 122 | 77 | 199 | 121 | 77 | 198 | 65 | 77 | 142 |
| | Localizer | 136 | 249 | 385 | 93 | 249 | 342 | 41 | 249 | 290 |
| Inner Marker (1000 ft) | Glideslope | 8 | 5 | 13 | 8 | 3 | 11 | 4 | 3 | 7 |
| | Localizer | 42 | 37 | 79 | 29 | 12 | 41 | 13 | 12 | 25 |

## LAAS NSE DERIVATION

The LAAS model used for this study is based on the Ground Accuracy Designator B (GADB) and Airborne Accuracy Designator A (AADA) models of LAAS, defined in [8] and developed by researchers at several institutions. The accuracy, integrity, continuity, and availability of the GADB/AADA model are likely to be slightly worse than the final Category I precision landing system supported by LAAS, so it represents a "worst case" LAAS NSE. The final NSE numbers were compared to a "best case" Category III model, GADC/AADB, to determine how inflated the final values may be. A derivation of the LAAS NSE model follows. For each case, a satellite elevation of 15 deg was used and only one ground reference receiver calculated the differential correction. Combining these assumptions gives a reasonable, but conservative value of NSE.

## AIRBORNE RECEIVER PSEUDORANGE ERROR MODEL

The airborne receiver's pseudorange error is modeled as the root sum square of the thermal noise (n) and airframe multipath errors (mp),

$$\sigma_{air} = \sqrt{\sigma_n^2 + \sigma_{mp}^2} \tag{5}$$

where, for $\theta = 15$ deg, (6)

$$\sigma_n(\theta) = a_0 + a_1 e^{-\theta/\theta_c} \tag{7}$$

and

$$\sigma_{mp}(\theta) = 0.13 + 0.53e^{-\theta/(10°)} \tag{8}$$

The coefficients for Eqn 7) are given in Figure 4 for the different airborne models.

Figure 4. Coefficients for the airborne receiver noise model

| Airborne Model | $a_0$ (m) | $a_1$ (m) | $\theta_c$ (deg) |
|---|---|---|---|
| AADA (worst) | 0.15 | 0.43 | 6.9 |
| AADB (best) | 0.11 | 0.13 | 4.0 |

## GROUND RECEIVER PSEUDORANGE ERROR MODEL

The ground reference receiver pseudorange error is modeled by

$$\sigma_{gr}(\theta) = \begin{cases} a_0 + a_1 e^{-\theta/\theta_c}, & \theta \geq 35° \\ \sigma_{max}, & \theta < 35° \end{cases} \tag{9}$$

where the coefficients are presented in Figure 5

Figure 5. Coefficients for the overall ground receiver pseudorange error model

| Ground station Model | $a_0$ (m) | $a_1$ (m) | $\theta_c$ (deg) | $\sigma_{max}$ |
|---|---|---|---|---|
| GADA (worst) | 0.50 | 1.65 | 14.3 | -- |
| GADC (best) | 0.15 | 0.84 | 15.5 | 0.24 |

## ATMOSPHERIC PSEUDORANGE ERROR MODELS

The troposphere and ionospheric pseudorange error models must be included in the LAAS NSE model and will be broadcast as part of the LAAS data link message. The tropospheric pseudorange error is modeled by

$$\sigma_{tropo} = \frac{\sigma_N h_0 \times 10^{-6}}{\sqrt{0.002 + (\sin\theta)^2}}\left(1 - e^{-\Delta h / h_0}\right) \quad (10)$$

where $\sigma_N = 30$, $\Delta h$ is the difference in height between the ground station antenna and the airborne antenna, $\theta = 15\ \text{deg}$, and $h_0$ may be calculated by

$$\begin{aligned} h_0 &= \frac{N_{dry} h_{0dry} + N_{wet} h_{0wet}}{N_R} \\ N_R &= N_{dry} + N_{wet} \\ N_{dry} &= \frac{77.6 P_s}{T_s} \\ N_{wet} &= 2.277 \times 10^4 \frac{RH}{T_s^2} 10^{\frac{7.4475(T_s - 273K)}{T_s - 38.3K}} \end{aligned} \quad (11)$$

$$\begin{aligned} h_{0dry} &= \frac{42700 - h_s}{5} \\ h_{0wet} &= \frac{13000 - h_s}{5} \end{aligned} \quad (12)$$

where $P_s$ is the atmospheric pressure in mbars, $T_s$ is the temperature in Kelvin, $h_s$ is the height of the ground station antenna above the ground, in meters, and RH is the relative humidity in percent. For this study, a sea level, standard pressure and temperature day was used for the atmospheric variables, 1013.8 mbars and 288 K, respectively. Relative humidity was 50%. The height of the LAAS reference antenna, $h_s$, was 2 meters above the ground.

## IONOSPHERIC MODEL

The ionospheric psuedorange error may be modeled by

$$\sigma_I = F_{pp} \frac{dI_v}{dx}(x_{air} + 2\tau_{air} v_{air}) \quad (13)$$

where $\frac{dI_v}{dx} = 4\text{mm/km}$, $x_{air}$ is the user to ground station distance, in meters, $\tau_{air} = 100\text{s}$ which is the airborne carrier-smoothing time constant, and $v_{air} = 70\text{m/s}$, the typical approach speed for a transport aircraft. The obliquity factor, $F_{pp}$, is approximated as

$$F_{pp} = \left[1 - \left(\frac{R_e \cos\theta}{R_e + h_I}\right)^2\right]^{1/2} \quad (14)$$

where $R_e$ is the earth's radius, 6378.1363 km, and $h_I$ is the height of the maximum electron density of the ionosphere, 350 km.

## SUMMARY OF PSEUDORANGE ERROR

The four components of the overall pseudorange error, airborne receiver thermal noise and multipath, ground receiver thermal noise and multipath, troposphere, and ionosphere errors are root sum squared to obtain the final, modeled pseudorange error

$$\sigma_{pr}(\theta, x_{air}, \Delta h) = \sqrt{\sigma_{air}^2 + \sigma_{grnd}^2 + \sigma_{tropo}^2 + \sigma_{iono}^2}$$

## PSEUDORANGE ERROR TO LATERAL NSE

To convert the pseudorange error into the position domain, the following equations are used

$$\begin{aligned} \sigma_{NSE}(x_{air}) &= \sigma_{pr}(x_{air}) \cdot \text{LDOP} \\ \text{LDOP} &= 0.818 \cdot \text{VDOP} \\ \text{VDOP} &= \frac{\text{VAL}}{5.8 \cdot \sigma_{pr}(7.5\text{km})} \end{aligned} \quad (15)$$

where VDOP is the vertical dilution of precision, VAL is the vertical alarm limit maximum of 10 meters and the denominator in the VDOP equation is the smallest error in the range domain that poses an integrity threat when converted to vertical position. The 0.818 factor in

the lateral dilution of precision (LDOP) equation comes from [9] and is a representative ratio between the standard deviations of the vertical and horizontal NSE components. The 7.5 km is a result of the approximate distance from the ground station to the runway threshold. This 7.5 km is then also added to the distance between the airplane and the runway threshold for purposes of computing lateral NSE. Figure 6 presents the lateral LAAS NSE for both models. The GADB/AADA model was used for the Monte Carlo simulations.

## NSE DISTRIBUTIONS

The Category II ILS FTE assumes the bias in the ILS installation has been calibrated to near zero or to the outside of the dual aircraft approach path. In the case of parallel runways, each with an ILS for guidance, each runway will produce a different NSE as each ILS installation is an independent guidance system. In the case of a single LAAS system serving multiple runways, the NSE will be approximately the same for each runway since the same GPS satellites will be used to create the differential corrections. It is assumed that both airplanes will be observing the same GPS satellites while on simultaneous approaches. The NSE distributions are presented in Figure 6.

Figure 6. LAAS and ILS NSE distributions

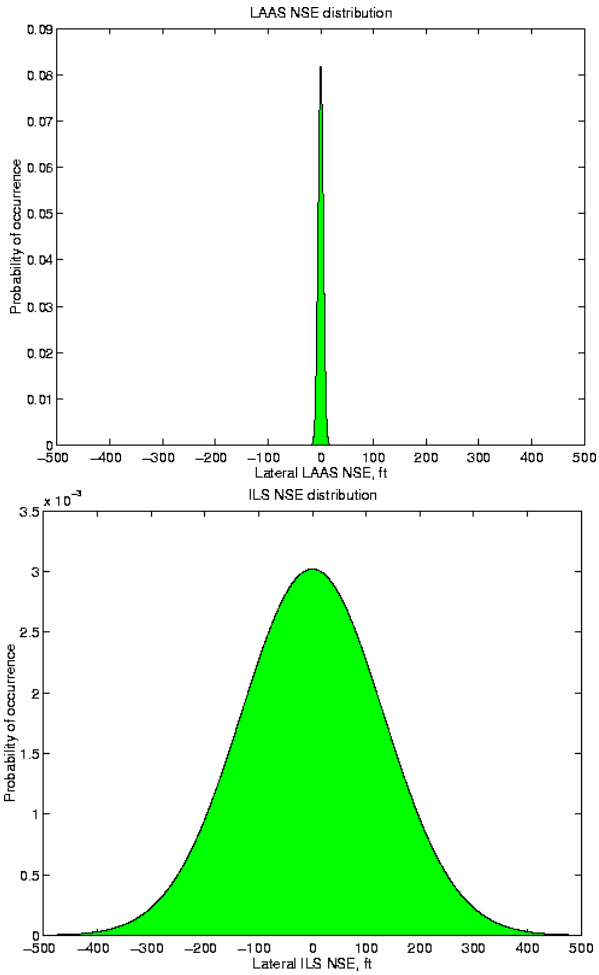


## FLIGHT TECHNICAL ERROR MODELS

The FTE models were based on demonstrated pilot-in-the-loop performance using a corridor approach path with a tunnel-in-the-sky as the pilot display [2] and the demonstrated NASA Langley B-757 auto-pilot performance while tracking a DGPS-generated angular approach path [10]. Use of the tunnel-in-the-sky presumes that LAAS is available to provide position and velocity information, an Attitude-Heading Reference System (AHRS) is available to provide pitch, roll, and yaw, and an Inertial Measurement Unit (IMU) is available to provide smoothing for the necessary high update rates. These additional system requirements thus precludes the use of the tunnel-in-the-sky with only an ILS for guidance. The one sigma value for FTE for the piloted case was 16 ft while the auto-piloted one sigma FTE was 11.9 ft, both in smooth air. Distributions of the FTE are presented in Figure 7. Note that FTE number currently used by industry and the FAA for similar calculations is approximately 700 ft.

Figure 7. Pilot and auto-pilot lateral FTE distributions

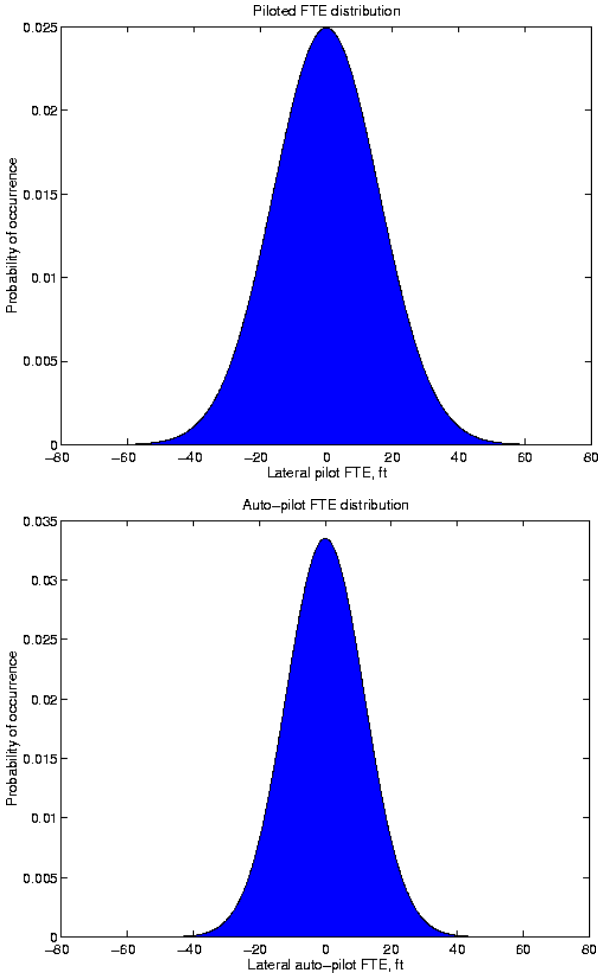


The NSE and FTE data are summarized in Table 8.

Figure 8. NSE and FTE for Monte Carlo study

| Parameter | 1σ value (ft) |
|---|---|
| Piloted FTE | 16 |
| Auto-pilot FTE | 11.9 |
| ILS NSE | 132 |
| LAAS NSE | 4.9 |

## DELAY MODELS

The following sources of delay were considered in the delay model: 1) data link update rate and collision detection and resolution time, 2) antenna/computer electronics delay, 3) pilot/auto-pilot response time, and 4) electro-mechanical actuator delay. Each of the components were determined to be either a fixed delay time or were assigned a uniform distribution based on experimental data or analysis.

## DELAY DUE TO ELECTRONICS AND ACTUATORS

The antenna/computer electronics delay and the electro-mechanical actuator delay were each assigned fixed quantities. These two quantities are based on known lags in computer processing times as well as actuator response times. Based on conversations held with personnel at the FAA Mike Munroney Aeronautical Center, the electronics delay was chosen to be 0.5 sec. The electro-mechanical actuator delay time, defined as the delay from the initial movement of the yoke to the onset of positive roll rate, was also estimated to be 0.5 sec.

## DELAY DUE TO DATA LINK AND COLLISION DETECTION

The data link update rate directly affects the collision detection algorithm as it contains the necessary information to estimate aircraft trajectories. To prevent a high probability of false alarms, it is estimated that at least two updates from “anomalous” adjacent airplanes states will be required before on-board collision detection algorithms will determine that an escape maneuver is required. Using one Hz ADS-B as the baseline data link, the minimum time to update the aircraft states twice is slightly over 1.0 sec, assuming the start of the blunder occurs just before an update. Note that this means the blundering aircraft could not have moved very far nor changed its velocity vector to any significant degree which implies that roll and roll rate may be required parameters in the data link in order to infer intent. However, as a minimum bound, the data link delay is estimated to be 1.0 sec. At a maximum, the onset of the blunderer’s roll rate will occur immediately after the transmission of the aircraft states, causing a delay of 2.0 sec due to the update rate. Although a higher update rate data link may be employed for UCSPA, the blundering aircraft must still have time to exhibit a trajectory change sufficiently severe to be called a blunder, so one to two seconds for the range of possible delay due to data link and collision detection is still considered reasonable.

## DELAY DUE TO THE PILOT OR AUTO-PILOT

For the cases with the auto-pilot coupled, not only is the auto-pilot coupled during the approach, but remains in control of the aircraft throughout the emergency escape maneuver. This is termed an “intelligent” auto-pilot. During this time, the pilot monitors the aircraft systems as is currently done during an approach. For the intelligent auto-pilot approach and escape maneuver, it is assumed that the auto-pilot has immediate access to the results of the collision detection algorithm and can react to an emergency escape maneuver in less than 100 msec. The auto-pilot must then either activate the yoke

or electronically signal the actuators to begin the escape maneuver. Moving the yoke causes more delay than directly signalling the actuators, so this case is modeled by a 0.5 sec delay, for a fixed delay time of 0.5 sec due to the auto-pilot.

Data from NASA Langley's AILS flight tests [5] demonstrated an average pilot response time of 0.3 sec to a computer generated collision alert during simulated IMC with a 2500 ft separation distance, with a maximum response time of 1.0 sec. Average reaction times demonstrated in the simulator studies of [11] were 0.84 sec for the same scenarios of the flight test, with a maximum of 1.84 and a minimum of 0.12 sec, demonstrating that more than displays and aural warnings impact the human in the loop. Experimental results from [3] for a pilot out-the-window visual determination of an aircraft maneuver at less than 2000 ft separation measured a maximum pilot delay time of 2 sec for a roll maneuver. This includes the delay from yoke movement to control surface actuation. Based on this data, a uniform delay distribution ranging from 0.3 to 2.0 sec was used as the model for delay due to the pilot.

A summary of the components of the total delay distribution is presented in Figure 9. Either the auto-pilot or the pilot reaction time is used in each simulation; they are not used together.

Figure 9. Components comprising the total delay distributions

| Parameter | Delay (sec) |
|---|---|
| Antenna/computers (fixed) | 0.5 |
| Electro-mechanical actuators (fixed) | 0.5 |
| Pilot Reaction Time (uniform distribution) | 0.3 to 2.0 |
| Auto-pilot Reaction Time (fixed) | 0.5 |
| Data Link/collision detection delay (uniform distribution) | 1.0 to 2.0 |

## LONGITUDINAL POSITION DISTRIBUTION

Videotaped observations of simultaneous, visual parallel approaches into San Francisco airport made by this author demonstrated that the longitudinal spacing can vary widely from approach to approach. Often, the approaches resembled dependent approaches (diagonal spacing 2 nm or more) rather than simultaneous approaches. Although future auto-pilots may have the precision necessary to bring two aircraft to positions exactly abeam each other, it is likely that there will be some permitted longitudinal position variation. For this study, a uniform longitudinal distribution of +/- 500 ft was used for the initial position of the blundering aircraft at the start of the blunder.

## AIRSPEED DISTRIBUTION

So as not to limit the study to exactly matched aircraft, the relative velocity of the evading aircraft was modeled as a uniform distribution with values between +/- 20 kts from that of the blundering aircraft at the start of the blunder. This variation accounts for differing approach speeds.

## SUMMARY OF MONTE CARLO PARAMETERS

For each simulation run, the following variables were randomly sampled from either a gaussian or uniform distribution, as described in the preceding sections:

- Flight technical error for each aircraft
- Navigation sensor error for each aircraft
- Pilot reaction time
- Data link/collision detection delay time
- Longitudinal relative position
- Relative airspeed

The following deterministic variables were set at the values given in the baseline trajectory described in [1]:

- Blunderer airspeed (140 kts)
- Maximum roll rate (10 deg/s each)
- Maximum roll angle (30 deg each)
- Maximum heading change (30 deg blunderer, 45 deg evader)
- Actuator and antenna delay time (1.0 sec)
- Auto-pilot reaction time (0.5 sec)

## MONTE CARLO RESULTS

At each runway spacing of 750, 1100 and 1500 ft, 100,000 trajectories were run with the distributions described in the previous sections. For each trajectory, the closest point of approach was calculated and if this distance was less than the B-747 fuselage length, this was counted as a collision. At the end of the 100,000 runs, the total number of collisions was divided by the total number of runs, resulting in the Probability of Collision During a Blunder for that runway spacing. Figure 10 presents the results of the Monte Carlo runs for the various configurations and defines the three cases: A, B, and C. A plot of the probability of collision versus runway spacing for each case is presented in Figure 11.

.

Figure 10. Probability of collision during a blunder. 95% confidence interval is +/- 0.3%

| | Piloted with tunnel-in-the-sky guidance FTE 1σ =16ft delay=0.3 to 2.0 sec | Intelligent auto-pilot with auto-escape FTE 1σ =11.9ft delay = 0.5 sec | LAAS 1σ = 4.9ft | ILS 1σ = 132ft | P(collision) 750 ft | P(collision) 1100 ft | P(collision) 1500 ft |
|---|---|---|---|---|---|---|---|
| Case A | X | | X | | 5.857% | 0% | 0% |
| Case B | | X | X | | 0.001% | 0% | 0% |
| Case C | | X | | X | 8.9940% | 0.17% | 0% |

Figure 11. Probability of collision during a 30 deg blunder for various sensor/pilot combinations

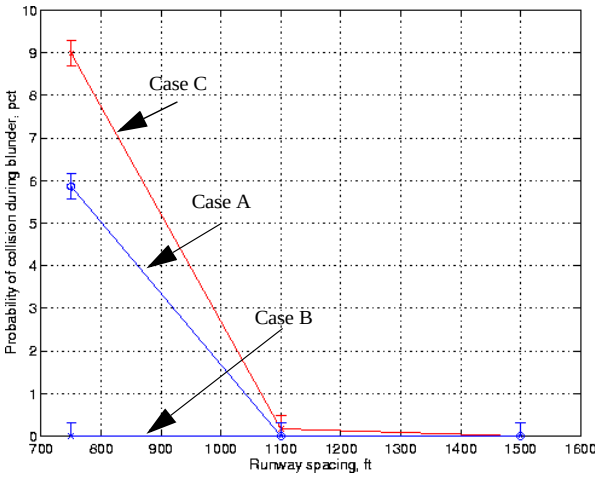


It must be emphasized that additional onboard equipment is required for each case, as well as presumed enhancements to the existing GPS system, as discussed in previous sections. In summary,

•the piloted cases assume:

- tunnel-in-the-sky guidance, which currently relies upon LAAS for position and velocity, an AHRS for attitude information, and an IMU for smoothing position, velocity, and attitude.

- full state information on the adjacent aircraft along with collision detection ability

•the auto-piloted cases assume:

- computerized collision detection and resolution with the auto-pilot in control throughout all maneuvers

- full state information on the adjacent aircraft

## ACCURACY OF THE MONTE CARLO SIMULATION

Because the probability of collision during a blunder calculation is a binomial random variable (it either collides or it does not), the Central Limit Theorem theorem may be used for large numbers of trials to make a Gaussian approximation to the 95% confidence interval around the calculated probability of collision. The binomial random variable is a sum of independent, identical Bernoulli random variables [12] with finite mean and variance and in the limit, the Bernoulli cumulative distribution function approaches that of the Gaussian. For the 100,000 total runs, in each case the 95% confidence interval that P(collision) is the true value is +/- 0.3103%. The relationship between confidence interval and error bound is presented in Figure 12.

Figure 12. Confidence interval vs. error for 100000 Monte Carlo simulations

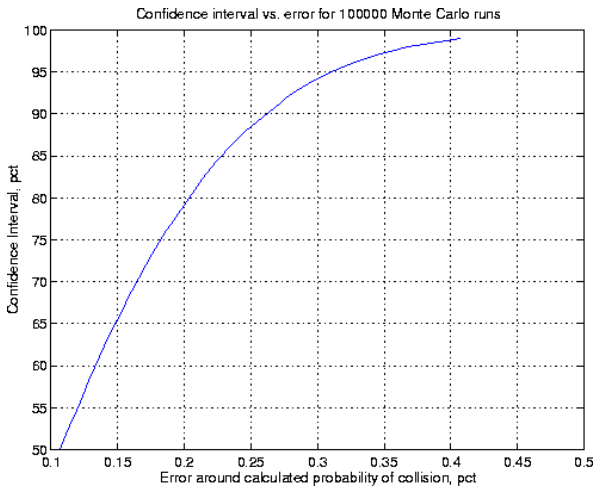


## RESULTS OF THE PROBABILITY OF COLLISION DURING A BLUNDER

Using today's ILS, the probability of collision during a 30 deg blunder is 9% with 750 ft runway separation, even assuming the best possible guidance system in the aircraft and advanced data links providing excellent information on the neighboring traffic. This is clearly unacceptable and illustrates one of the reasons why closely spaced approaches are not possible with ILS

providing the navigation. Increasing the runway spacing to 1100 ft yielded 170 collisions during a blunder out of 100,000 trials when using the ILS, which is still problematic. However, it appears from the study that 1100 ft spacing would be acceptable if navigation is provided by a system with the accuracy of LAAS. The airplanes may be manually flown with advanced displays or the "intelligent auto-pilot" may be engaged, however; the airplanes are required to be equipped with an advanced data link that provides the position, velocity, roll angle, and roll rate of the neighboring traffic. In order to achieve a low probability of collision during a blunder (0.01%) at a runway spacing of 750 ft, it is necessary to use the intelligent auto-pilot to reduce reaction time, LAAS for low NSE and TSE, and the advanced data link, which provides complete information on the adjacent traffic.

## ULTRA CLOSELY SPACED PARALLEL APPROACH SAFETY

Using the results of the Monte Carlo simulation and an estimate of the current safety level for instrument approaches, one may calculate the acceptable blunder frequency for ultra closely spaced parallel approaches. According to the FAA, if this blunder frequency is less than an intuitively reasonable number, then ultra closely spaced parallel approaches may be conducted with acceptable risk levels.

In the Precision Runway Monitor program, the FAA adopted the following methodology for estimating the acceptable blunder rate [13,14]:

From data obtained between 1983 to 1988, there were two accidents during an estimated total of five million approaches. This reduces to an accident rate of one per 2.5 million approaches. Since two airplanes are on approaches during a UCSPA, one UCSPA counts as two approaches.

The FAA identified nine potential causes of accidents during a final approach and added a blunder during a PRM approach as a tenth. Thus, if the current accident rate of one per 2.5 million approaches is to be maintained, it was approximated that a blunder contributes one tenth toward that accident rate. Therefore, the accident rate due solely to blunders during a PRM may be no greater than one per 25 million.

One key assumption the FAA made for this analysis was that out of 100 blunders occurring during a PRM approach, 99 of them were "recoverable", meaning that the final approach monitor identified and the pilot corrected the blunder before requiring the adjacent airplane to perform an emergency escape maneuver. No data was presented to support this assumption and the blunder recovery for a UCSPA may not be as high, however; for the sake of similarity, this analysis will use the 99% blunder recovery rate.

With these assumptions and data, the total number of allowable blunders may be written as

$$\left(\frac{1\text{ accident}}{25e6\text{ approaches}}\right)\left(\frac{100\text{ total blunders}}{1\text{ bad blunder}}\right)\text{x}$$
$$\left(\frac{\text{bad blunder collision rate}}{2\text{ accidents}}\right)\left(\frac{2\text{ approaches}}{1\text{ UCSPA}}\right) \quad (16)$$

where a "bad blunder" is defined as the sustained, 30 deg blunder discussed in the previous sections and the "bad blunder collision rate" is determined from the aforementioned Monte Carlo simulations. If one inserts the "bad blunder collision rate" for the LAAS/auto-pilot configuration at 750 ft runway spacing, the result is

$$\left(\frac{1\text{ accident}}{25e6\text{ approaches}}\right)\left(\frac{100\text{ total blunders}}{1\text{ bad blunder}}\right)\text{x}$$
$$\left(\frac{333\text{ bad blunders}}{2\text{ accidents}}\right)\left(\frac{2\text{ approaches}}{1\text{ UCSPA}}\right) \quad (17)$$
$$= \frac{1\text{ total blunder}}{750\text{ UCSPA}}$$

where the 333 "bad blunders" is calculated from the upper end of the confidence interval on the probability of collision of 0.3%:

$$\text{P(collision)} = \frac{3\text{ collisions}}{1000\text{ bad blunders}}$$
$$\text{bad blunder collision rate} = \frac{1000\text{ bad blunders}}{3\text{ collisions}} \quad (18)$$
$$= 333\frac{\text{bad blunders}}{\text{collision}}$$

This result of Eqn 17) means that 750 blunder-free UCSPAs must occur before one blunder is allowed. Obviously, the higher the denominator, the more blunder-free approaches must occur and the higher the safety level. Using the resultant permissible blunder rate in Eqn 17), if San Francisco has 5,000 ultra closely spaced parallel approaches a year, six blunders are permissible to stay within the existing safety levels. We may fill out the rest of the test matrix given the probabilities in Figure 10. Figure 13 uses Eqn 17) to calculate the number of blunder-free UCSPAs flown before a blunder may

occur. The numbers in this table are the number of blun-

Figure 13. Number of blunder-free UCSPAs, given the P(collision) in Table 10

| | Piloted with tunnel-in-the-sky guidance FTE $1\sigma$ =16ft delay=0.3 to 2.0 sec | Intelligent auto-pilot with auto-escape FTE $1\sigma$ =11.9ft delay = 0.5 sec | LAAS $1\sigma$ = 4.9ft | ILS $1\sigma$ = 132ft | No. of safe UCSPA 750 ft | No. of safe UCSPA 1100 ft | No. of safe UCSPA 1500 ft |
|---|---|---|---|---|---|---|---|
| Case A | X | | X | | 14,500 | 750 | 750 |
| Case B | | X | X | | 750 | 750 | 750 |
| Case C | | X | | X | 22,500 | 750 | 750 |

der-free approaches that must occur in order to maintain acceptable safety levels. Note that the 750 appearing in several columns is not related to the runway spacing, but results from the confidence interval of 0.3% and the resulting probability of collision rate. Based on [13], the maximum permissible number of blunder-free approaches required by the FAA is 2,000, which means that all three navigation system/pilot configurations are acceptable at 1100 and 1500 ft runways spacings. Only the LAAS/auto-pilot combination gives acceptable performance at 750 ft separation.

## CONCLUSIONS

This analysis demonstrates that ultra closely spaced parallel approaches are technically achievable using upcoming advanced navigation systems, data links and pilot interfaces. The existing runway spacing requirement of 4300 ft or 3400 ft may be substantially reduced, to the levels of 1100 or 1500 ft, based on the FAA minimum safety requirements for a multi aircraft instrument approach. The critical underlying technical presumptions of this research, differential GPS, air-to-air and air-to-ground data links, and a good auto-pilot or pilot interface, have all been successfully demonstrated in flight test by either this researcher or other researchers. Yet to be designed and tested is an intelligent auto-pilot that autonomously executes the emergency escape maneuver without pilot intervention. At least one collision detection algorithm has been successfully flight tested and several are in work. Most of these algorithms assume aircraft attitude as well as three dimensional position and velocity will be available in the data link. Given the tight requirements on minimizing the response time of the evading aircraft during a blunder, the collision detection community may well require a data link update rate greater than one Hz in order to provide adequate collision diagnosis during an ultra closely spaced parallel approach while minimizing the false alarm rate. A summary of the components required to achieve 750 and 1100 ft runway separations for two nominal B-747 aircraft within the acceptable FAA safety margins is presented in Figure 14.

Figure 14. Minimum component requirements for 750 and 1100 ft runway spacing

| Navigation Sensor | Human-machine interface | Traffic information required | Minimum runway spacing |
|---|---|---|---|
| Cat I LAAS | Tunnel-in-the-sky (requires LAAS, AHRS, and an IMU), pilot in the loop | Full state information on adjacent traffic (position, velocity, attitude) | 1100 ft |
| Cat I LAAS | Intelligent auto-pilot in control throughout approach and escape maneuver | Full state information on adjacent traffic (position, velocity, attitude) | 750 ft |

The technology for UCSPA will require new equipment in aircraft and on the ground. It will be such that both aircraft on a simultaneous approach will need to be equipped with the new technology which means that most aircraft using an airport will need to be equipped in order to reap the full capacity benefits. The equipment will probably cost on the order of $200K per aircraft. The airframe manufacturers and their airline customers would prefer that airports foot the bill for wider runway spacing, thus not requiring expensive aircraft re-equi-

page. However, a wider view is necessary for the best overall solution for the taxpayers, the airline passengers, and freight shippers who ultimately have to pay for the full system costs including airport expansions. The wider view also should take into account the welfare of airport neighbors, residents of areas that might become new airports, and the environmental damage brought by expanding airports into areas that are now water. To put this into perspective, the re-equipage of 10,000 aircraft (the current U.S. commercial fleet) would cost approximately $2B whereas the expansion of SFO into the bay for new runways is projected to cost more than $2B! And this is just one proposed airport expansion project. In short, development of technology that allows the use of very closely spaced runways in instrument conditions has huge long-term environmental and cost benefits. Development and flight test to validate hardware designs for pilot and air traffic control acceptance should be a high priority for the FAA, NASA, and the avionics manufacturers.

## ACKNOWLEDGEMENTS

The authors would like to thank Prof. Claire Tomlin and Rodney Teo for their helpful discussions on ultra closely spaced parallel approaches. In addition, the partial financial support of this research from Zonta International and the American Association of University Women is greatly appreciated.

## REFERENCES

[1] Houck, S. and Powell, J.D., "A Parametric Sensitivity Study of Ultra Closely Spaced Parallel Approaches", Proceedings of the Digital Avionics Systems Conference, Philadelphia, PA, 2000. http://waas.stanford.edu

[2] Houck, S., et al., "Flight Test of WAAS for Use in Closely Spaced Parallel Approaches", Proceedings of the Institute of Navigation's GPS Conference, Nashville, TN, 1999. http://waas.stanford.edu

[3] Houck, S. and Powell, J.D., "Visual, Cruise Formation Flying Dynamics", AIAA 2000-4316, Proceedings of the AIAA Atmospheric Flight Mechanics Conference, Denver, CO, 2000.http://waas.stanford.edu

[4] Abbott, T., et al, AIAA-2000-4358, Proceedings of the AIAA Guidance, Navigation and Control conference, Aug 2000, Denver, CO.

[5] Nelson, Robert C., "Flight Stability and Automatic Control", 2nd edition, McGraw Hill, 1998.

[6]US Standard Flight Inspection Manual, FAA Order 8200.1A, May 1996, revised July 2000.

[7]Kayton, M. and Fried, W., "Avionics Navigation Systems", Wiley Interscience, 2nd edition, 1997.

[8]McGraw, G., Murphy, T., Brenner, M., Pullen, S., Van Dierendonck, A., "Development of the LAAS Accuracy Models", presented at the Institute of Navigation's GPS conference, Sep 2000, Salt Lake City, UT

[9]Nam, Y., Zalesak, T., Clark, B., Murphy, T., Anderson, L., and DeCleene, B., "A GBAS Landing System Model for Cat I", proceedings of the IAIN World Congress, June 2000, San Diego, CA

[10] Technical correspondence with NASA Langley

[11]Abbott, T., Airborne Information for Lateral Spacing, preliminary report on simulation studies, NASA Langley, August 2000.

[12]Leon-Garcia, A., "Probability and Random Processes for Electrical Engineering", Addison Wesley publishers, second edition, 1994.

[13]Lankford, McCartor, Yates, Ladecky, and Templeton, "Comparative Study of Airborne Information Lateral Spacing (AILS) System with Precision Runway Monitor System", DOT-FAA-AFS-420-83, April 2000.

[14]Precision Runway Monitor Demonstration", DOT/FAA/RD-91/5, February1991.